Synthesis of Nanostructured Copper-doped Titania and Its Properties

Oman Zuas*,   Harry Budiman

Abstract: Nanostructured pure-TiO$_2$ and Cu3%-TiO$_2$ were successfully synthesized via co-precipitation method. The X-ray diffraction (XRD) result proves that the synthesized sample were predominantly in anatase phase with size in the range of 8∼16 nm, which are in good agreement with the transmission electron microscopy data. Owing to doping of copper, not only did the thermal stability of the TiO$_2$ decrease, but also a significant decrease in its particle size and a shift of the adsorption edge to a higher wavelength region appear. The activity of both pure-TiO$_2$ and Cu3%-doped TiO$_2$ was tested to study their ability to decolorize congo red (CR) dye in aqueous solution. We observed that the CR dye was decolorized faster by Cu3%-TiO$_2$ than pure-TiO$_2$. Results of this study demonstrate a potential application of the synthesized sample for decolorizing dye pollutants from aqueous waste.

Keywords: Nanostructure; Copper; Titania; Decolorization; Congo red

Introduction

In 1972, titanium dioxide (TiO$_2$) was firstly discovered by Fujishima and Honda as an active photocatalyst [1]. Since then, TiO$_2$ has became one of the most important semiconductor materials in daily life, moreover, it has been widely used in fuel cell, solar energy conversion, photocatalysts/catalyst for environmental remediation processes, white pigment in paints and paper, bone implant material, ultra-violet (UV) absorber in sunscreen cream and other cosmetic products, and additive in food products [2-5]. Such wide range of application is quite reasonable, because TiO$_2$ is an inexpensive, environmentally friendly material with high chemical stability, high mechanical strength and photo activation [6-8]. However, exploring the properties of TiO$_2$ for improving its efficiency is still an emerging area of research. In this regards, modifications of instrinsic properties of TiO$_2$ by doping with other oxide semiconductor such as Al$_2$O$_3$ [9], CeO$_2$ [10], CuO [11],

Fe$_2$O$_3$ [12], SnO$_2$ [13], SiO$_2$ [9,14], WO$_3$ [15], ZnO [16] and ZrO$_2$ [9,14] have long been proposed. Specially, copper (Cu) was found to be one of the most considerable element among those oxide semiconductors because of its notable effects on the activity of TiO$_2$. Numerous works on the applications of Cu-TiO$_2$ have been reported in the areas of solar energy [17], environmental remediation for chemical contaminants removal [18-24], and microbial treatment [25,26]. In the area of solar energy, the presence of Cu element significantly extends the light response of TiO$_2$ into the visible region, which further enhance the photoelectochemical properties of the TiO$_2$ [17], and increase the activity of the TiO$_2$ as catalyst for hydrogen generation [22]. The Cu was also found to be a promising dopant to increase the properties of TiO$_2$ for converting carbon dioxide to higher carbon compounds [18-20] and for generating hydrogen from water [21]. In the field of microbial treatment, the Cu species can be used as an impurity material to enhance the TiO$_2$ activity for the treatment of water con-

Research Center for Chemistry (RCChem), Indonesian Institute of Sciences (LIPI), Kawasan PUSPIPTEK Serpong, 15314, Tangerang, Banten, Indonesia
*Corresponding author. E-mail: oman.zuas@lipi.go.id (Official), oman.zuas@yahoo.co.id (General)

taining harmful biological contaminants [25,26]. Thus, it is evident that the existence of Cu species at TiO_2 matrix plays an important role on the activity, because Cu could influence the particle size [20,23], and optical or electronic properties of TiO_2 [17,21], as well as the number of oxygen or intermediate species on the surface of the TiO_2 [22,27]. Recently, in the area of environmental remediation for removal of chemical pollutants, materials having nano dimensional structure are still preferred because of the high surface area well-correlated to their small size [28-30], which grant them more adsorption site for better activity [31,32].

Despite the fact that the aims to improve the TiO_2 activity by doping with Cu have been pointedly achieved, most of those mentioned studies were conducted with light-assisted method. On the other hand, concerning the environmental remediation process for organic contaminant removal, a direct catalytic application of nanostructured TiO_2-based material in the absence of light assistance is still challenging. Therefore, in this study nanostructured pure TiO_2 and Cu3%-doped TiO_2 were synthesized, characterized and tested for their activity. The nanostructured samples were synthesis by co-precipitation method. The morphology and structure were characterized. The activity of the synthesized samples was evaluated for direct application to decolorize CR dyes, as the model compound, in aqueous solution through microwave-assisted catalytic reaction process in absence of the light assistance.

Experiment

Chemicals

All chemicals were purchased from commercially available sources and were used without further purification. The chemicals include Ammonia solution (NH_4OH, Merck, 25%), Cetyltrimethyl Ammonium Bromide (CTAB, Merck, 98%), Zinc chloride ($ZnCl_2$, Merck, 98%), Copper nitrate ($Cu(NO_3)_2 \cdot 3H_2O$, Merck, 99.5%), Titanium tetrachloride ($TiCl_4$, Merck, 98%), Congo red dye (Sigma, 97%), and purified water was produced from a NanoPure purification system (Millipore Corp., 17.5 MΩ·cm).

Synthesis of Nanostructured Pure-TiO_2 and Cu-TiO_2

Nanostructured copper-doped titania at 3 wt% level of copper (denoted as Cu3%-TiO_2) was synthesized using co-precipitation method with the same procedure as described in our previous study [33], except that copper was used as the metal dopant and a higher calcination temperature (500℃) was applied in present study. The procedure was as follows: A certain amount of copper precursor was dissolved in CTAB solution (0.2 M) un-

der stirring (600 rpm) for 5 min, giving a mixture sol.-A. The mixture sol.-A was stored in a refrigerator at 0℃ for further use. Subsequently, a certain amount of concentrated $TiCl_4$ solution was then slowly dropped into freezed mixture sol.-A, giving a mixture-solution B. After that, the mixture sol.-B was precipitated using NH_4OH solution (25%) in 5 ml/min of dropping rate, under stirring, until the pH value of the solution reached 10, then placed the solution at 55~60℃ under stirring for 6 h for aging, giving a mixture sol.-C. The wet solid precursor in mixture sol.-C was separated from the solution by centrifugation at 8000 rpm for 10 min. The wet solid precursors were dried at 100℃ for 12 h to produce dry solid precursors. The dry solid precursor was calcined at 500℃ for 4 h. The pure TiO_2 was also synthesized using the same procedure without addition of copper precursor.

Characterization

The thermal curves of thermo gravimetric analyzer (TGA) were obtained from freshly dried solid precursor using a TGA 2050 thermal gravimetry with temperature limit from 20~900℃ in air flow. All X-ray diffraction (XRD) patterns of the synthesized samples were recorded on a Rigaku X-ray at 40 kV and 100 mA with $CuK\alpha$ as the radiation source. The 2θ was scanned in the range from 25° to 70° at a speed of 1.2°/min. The average crystallite size of the synthesized samples was calculated from the full-width at half-maximum (FWHM) using Scherrer's formula [34]. The ultraviolet visible diffuse reflectance (UV-Vis DR) spectra were recorded on a Shimadzu UV2450 spectrophotometer equipped with an integrated sphere. The reflectance spectra of the sample were analyzed under ambient condition in the wavelength range of 300~700 nm. The measured reflectance spectra were transformed into Kubelka-Munk ($F(R)$) function using $(F(R)) = (1 - R)^2/2R$, where R is the reflectance value of the sample. The Fourier Transform Infrared Spectroscopy (FTIR) spectra of the synthesized samples in potassium bromide (KBr) media were recorded on a Shimadzu IR Prestige DSR-8000 spectrometer in the range from 500 cm^{-1} to 4000 cm^{-1} at a scanning rate of 4 cm^{-1}/min. The surface morphology images and energy dispersive X-ray (EDX) of the synthesized samples was observed from a Tecnai G2 F20 tansmission electron microscopy (TEM) at an accelerating voltage 200 kV. The TEM samples were prepared by firstly dispersed in ethanol and then deposited onto a 300 mesh copper grid after sonication.

Activity Testing

The synthesized samples were tested for their activity of decolorizing the congo red (CR) dye in an aqueous solution under microwave irradiation. The catalytic

experiments were carried out using a thermostatic microwave apparatus (Milestone Microwave Laboratory System, MLS 1200). The experimental conditions were as follows: 10 ml of CR solution with known initial concentration (10 ppm) and a certain amount of the synthesized samples were transferred into a teflon vessel, which was put into the microwave apparatus to start the catalytic experiment. The treated CR solution was then centrifuged at 2200 rpm for 5 min to separate the solution from the particles of the synthesized sample. The absorption of the CR in treated solution was measured using a Shimadzu 3501 UV-Vis spectrophotomer at maximum wavelength of 498 nm. The concentration of the CR in the remaining treated solution was calculated from their calibration curve. The calibration curve ($A=0.0679C+0.0262$) with $R^2=0.9969$, obtained from the maximal absorbancies of a series of CR solution (0-15 mg/l), abided by Lambert-Beer's law, was used to determine the CR concentration in the treated solution. The catalytic decolorization percentages of CR (%, Decolorization) is expressed as follows:

$$\%Decolorization = (C_0 - C_t)/C_0 \times 100$$

where C_o (mg/l) and C_t (mg/l) are the CR initial concentration and concentration after time t (min), respectively.

Results and discussion

The TGA thermogram of the synthesized samples are presented in Fig. 1. For TGA thermogram of pure TiO_2 samples, it can be seen that the first broad TGA exotherm peak at about 25~220℃ is attributed to the lost of residual organic solvent and physisorbed water. These first two peaks occur concurrently with a mass loss of 11%. The second broad TGA exotherm peak in the range of 220~550℃ indicates decomposition of hydroxyl groups and organic molecules chemically bonded to the surface of TiO_2 sample, giving a further mass loss of 9%. In addition, a broad exotherm TGA in the range of 550~900℃ is obviously observed with a mass loss of 3%. After that, there is no mass loss for the TiO_2 sample and it may be assumed that TiO_2 amorphous phase has changed to TiO_2 crystalline phase. The total mass loss for the pure TiO_2 sample heated to 900℃ was about 23%. Similarly, the trend is found for Cu3%-TiO_2 sample as shown in Fig. 1. Lost of residual organic solvent and physisorbed water from the Cu3%-TiO_2 sample corresponds to TGA exotherm peak in the range of 50~260℃, resulting a mass loss of 11%. A TGA exotherm peak is also observed in the range of 260~540℃ which occur concurrently with a TGA mass loss of 20%, ascribing to the decomposition of hydroxyl groups and organic molecules. The formation of crystalline phase of Cu3%-TiO_2 sample is indicated by no TGA exotherm peak in the temperature range of

540~900℃. From the TGA thermogram properties, it may be concluded that the presence of copper in TiO_2 matrix has obviously influenced the thermal property of the TiO_2. One can notice that, the pure TiO_2 was more stable upon heating with smaller mass loss compared to Cu3%-TiO_2, giving the following order: pure TiO_2 (23% mass loss) >Cu3%-TiO_2 (35% mass loss). In other words, the thermal stability of TiO_2 has significantly decreased after copper doping.
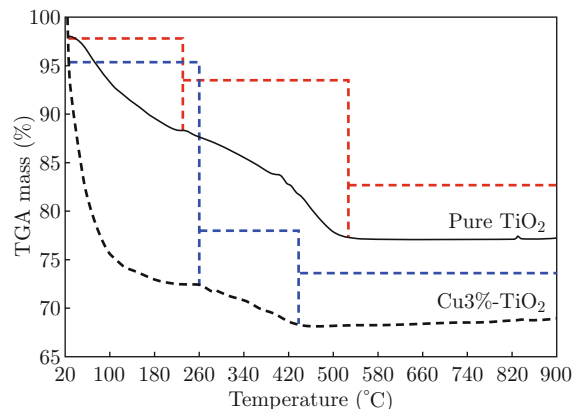

Fig. 1   TGA thermograms of the synthesized samples.

Figure 2 presents the XRD pattern of the synthesized samples. The well-defined diffraction peaks with 2θ are at about 25°, 38°, 48°, 54°, 55°, 63°, and 69°, which are assigned to the (101), (004), (200), (105), (211), (204) and (116) crystal plane, respectively. This XRD characteristic pattern is consistent with the standard JCPDS values of anatase TiO_2 (JCPDS Card No. 21-1272) [35-37]. No peaks for copper can be observed, which indicates the metal content added during the synthesis process was too low or the metal has been well-dispersed at TiO_2 matrix in the form of small cluster. The average crystallite size of the nanocomposite samples were calculated from the FWHM of anatase (101) reflection plane (Fig. 2(b)) using Scherrer's formula [38],

$$D = k\lambda/\beta \cos \theta$$

where D is the crystallite size, k is a constant (=0.9, assuming that the particles are spherical), λ is the wavelength of the X-ray diffraction. β is the FWHM and θ is the angle of diffraction. From the calculated crystallite size, it was found that the synthesized samples had small crystallite size with an average size of 15 nm and 9 nm for the pure TiO_2 and Cu3%-TiO_2, respectively. From this point, it can be noticed that the addition of copper decreased the crystallite size of the TiO_2 to some extent. Decrease in the particle size of TiO_2 might be ascribed to a broadening effect due to incorporation of the metal oxides into TiO_2 matrix [39], as can be seen by comparing the (101) reflection plane of pure TiO_2 with Cu3%-TiO_2 (Fig. 2(a)). Lowering the intensity and broadening the width of the (101) reflection

plane led to a decrease in the calculated crystallite size correspondingly. Moreover, the (101) reflection plane of the Cu3%-TiO$_2$ samples shifted to higher diffraction angle relative to pure TiO$_2$ (Fig. 2 (b)), implying an incorporation effect of copper at the TiO$_2$ lattice as Ti^{4+} position may be substituted by copper due to the similarity of their ionic radii (Ti=0.68 Å and Cu = 0.72 Å) [40].
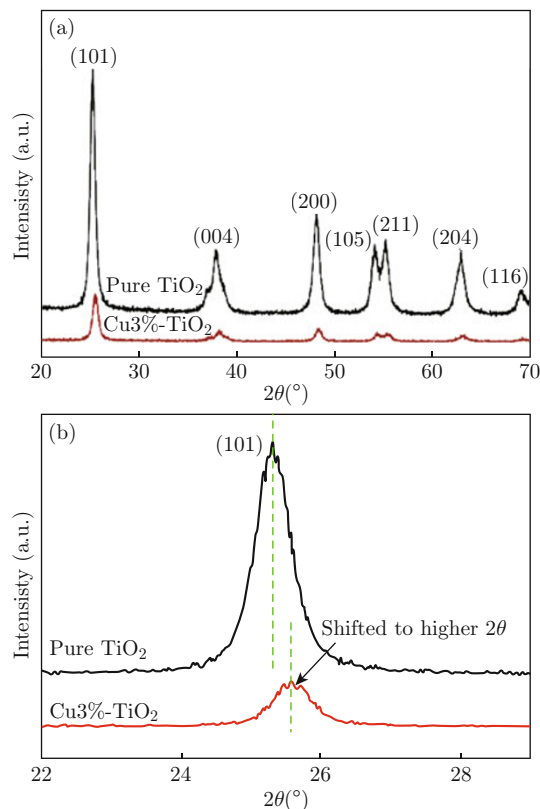

Fig. 2   XRD patterns of (a) the synthesized samples; (b) the (101) reflection plane of pure TiO$_2$ and Cu3%-TiO$_2$.

Figure 3 shows the UV-Vis DR spectra of the pure TiO$_2$ and Cu3%-TiO$_2$ samples. As can be observed from the spectra, a strong absorption peaks at around 350 nm is ascribed to the TiO$_2$ system, which decreases after Cu loading. A new strong absorption band between 350∼500 nm might be assigned to the presence of Cu species in the Cu3%-TiO$_2$ sample. In addition, The Cu-species also induced the formation of impurity inside the TiO$_2$, resulting in a shift of adsorption edge to higher wavelength region (red shift), which is characteristic for the TiO$_2$-system after metal doping.

The FTIR spectra of the synthesized samples were obtained in the scanning range of 500∼4000 cm^{-1}. As shown in Fig. 4, the spectra of pure TiO$_2$ before calcination clearly shows the bands (between 3500 and 3150 cm^{-1}), which correspond to H-bounded hydroxyl groups. It also shows significant peaks at about 2920 and 2850 cm^{-1}, which can be assigned to the C-H symmetrical and C-H asymmetrical stretching vibration

from the remaining organic-moiety [41], these peaks would disappear from the surface of all synthesized samples after heating treatment. The bending vibration mode of O-H is marked by peak at about 1628 cm^{-1} for all samples except for Cu3%-TiO$_2$ [14]. A clear peak at about 1456 cm^{-1} can be ascribed as a bending vibration mode of the N-H band from the CTAB [14]. However, the N-H bending vibration is not marked on the calcined samples.
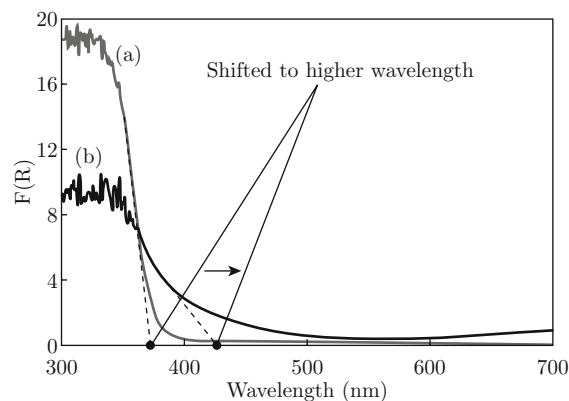

Fig. 3   UV-Vis diffuse reflectant spectrum of (a) pure TiO$_2$; (b) Cu3%-TiO$_2$ samples.
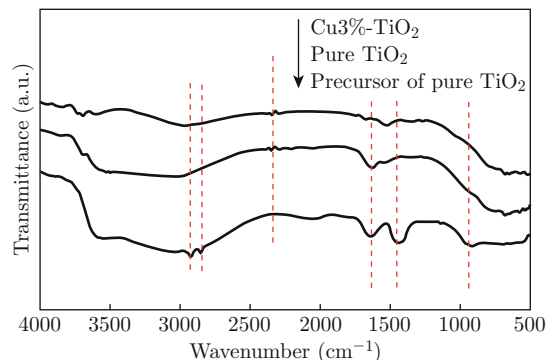

Fig. 4   The FTIR spectra of the synthesized samples.

TEM was used to further examine the particle size, crystallinity and morphology of the synthesized samples as shown in Fig. 5. From this figure, it can be seen that all synthesized samples display similar cluster morphology with estimated average size of the primary particles in the range of 8∼16 nm, which is in good agreement with the value determined by XRD data. It was also observed that all synthesized samples were present in pure anatase phase, which is indicated by no shuttle-like morphology for rutile phase. The lattice fringes, as shown in inset of Fig. 5, indicated that the particles are in good crystalline nature. The EDX result demonstrates the present of C, O, and Ti element in the pure TiO$_2$ sample (Fig. 6(a)), except for Cu which is also present in Cu3%-TiO$_2$ sample (Fig. 6(b)).
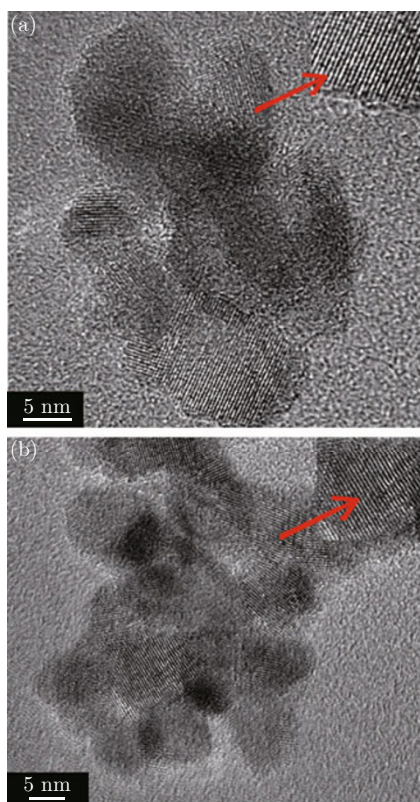
Fig. 5 The high resolution TEM images of (a) pure TiO$_2$; (b) Cu3%-TiO$_2$ (inset: lattice fringer).
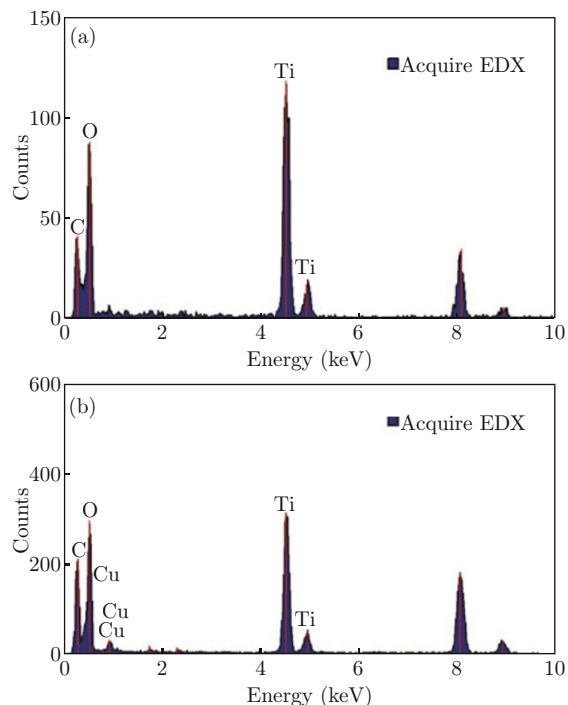

Fig. 6 The EDX spectra of (a) pure TiO$_2$; (b) Cu3%-TiO$_2$.

The performance of the synthesized samples were tested for microwave-assisted catalytic decolorization of CR synthetic dye in aqueous solution. Figure 7

shows both the absorption spectra of CR as a function of time during the catalytic decolorization process with pure TiO$_2$ and Cu3%-TiO$_2$. Obviously, the absorbance intensity of CR that were obtained over pure TiO$_2$ (Fig. 7(a)) slowly decreased with passage of time. In contrast, the absorbance intensity of the CR over Cu3%-TiO$_2$ (Fig. 7(b)) rapidly decreased and the absorption band disappeared after the first minute. The absorbance curve indicates that the CR dye was decolorized slower over pure TiO$_2$ than that of Cu3%-TiO$_2$. Inset of Fig. 7 represents the change in color of the dye during the microwave-assisted catalytic decolorization process.
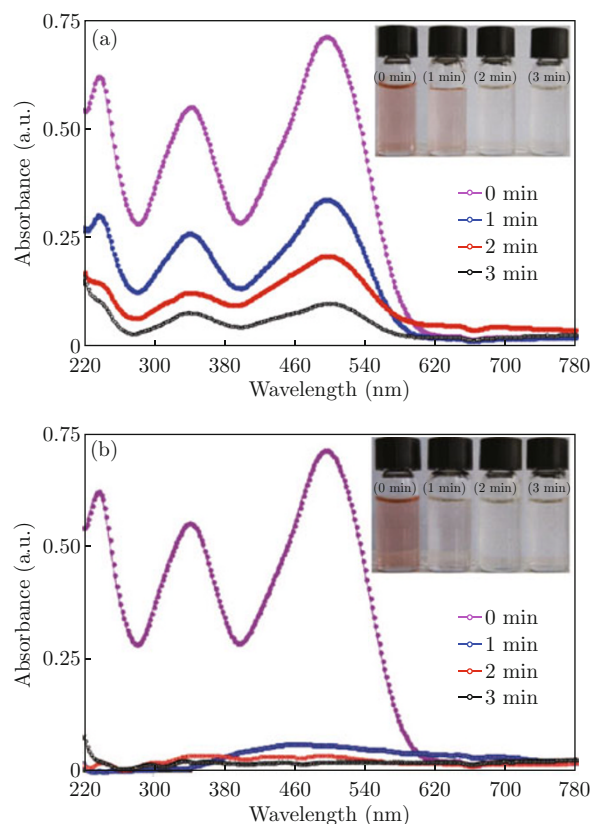

Fig. 7 UV-vis spectra profiles of CR dye during the microwave-assisted catalytic decolorization over (a) pure TiO$_2$ sample; (b) Cu3%-TiO$_2$ (conditions: intial CR concentration = 10 ppm, catalyst dosage = 2.5 g/l, microwave power 300 W).

Figure 8 shows a curve of percent decolorization of the CR during the microwave-assisted catalytic process over pure TiO$_2$ and Cu3%-TiO$_2$. As can be seen in the curve, 53% of CR dye was decolorized by the pure TiO$_2$ in the first minute. Furthermore, the decolorization process gradually increases as time prolongs. The CR dye was almost decolorized completely after an interval of 6 min with a maximum decolorization percentage of 97%. In case of decolorization of CR dye over Cu3%-TiO$_2$, the CR dye was decolorized rapidly. It took

only 1 min to decolorize 90% of the CR dye. Furthermore, the decolorization process was completed in 2 min where almost 100% of CR disappeared. Considering the decolorization efficiency of pure TiO_2 and Cu3%-TiO_2 after being microwave-assisted catalysis for 2 min, it is evident that the Cu3%-TiO_2 showed a greater of decolorization ability than that of pure TiO_2. This may be due to the Cu3%-TiO_2 sample which has smaller particle size compared to that of pure TiO_2. As the smaller the crystallite size, the larger the surface area, which further enables the synthesized sample to have more adsorption site and, an increased surface contact of CR-catalyst which, further promote the fast decolorization process under microwave irradiation. However, more detailed study to understand the performance and mechanism of catalytic process over pure TiO_2 and Cu3%-TiO_2 under microwave assistance is required.
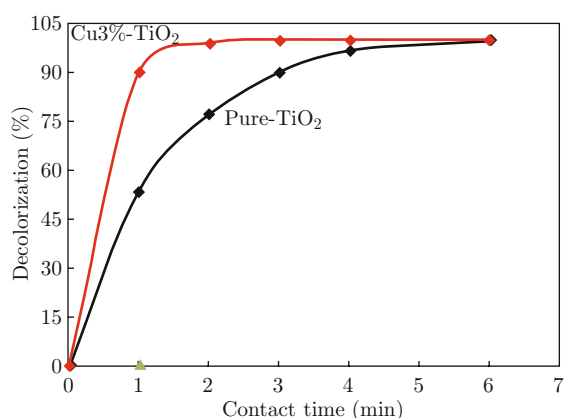

Fig. 8   Percent decolorization of CR as a function of time (min) (conditions: initial CR concentration = 10 ppm, catalyst dosage = 2.5 g/l, microwave power 300 W).

Conclusion

Nanostructured pure-TiO_2 and Cu-doped TiO_2 have been synthesized by using co-precipitation method. The presence of the copper dopant at TiO_2 matrix not only influenced the thermal stability of the TiO_2 but also decreased the particle size of the TiO_2. The catalytic activity of Cu3%-TiO_2 was higher than that of pure TiO_2. It can be assumed that the smaller particle size of Cu3%-TiO_2 may play an important role for its high activity. The smaller crystallite size which will cause the larger surface area results in the rapid decolorization process over the nanostructured Cu3%-TiO_2. However, more detailed study to understand the activity performance of the synthesized sample is essential.

Acknowledgements

References

[1] A. Fujishima and K. Honda, "Electrochemical photolysis of water at a semiconductor electrode", Nature 238, 37-38 (1972). http://dx.doi.org/10.1038/238037a0

[2] O. Carp, C. L. Huisman and A. Reller, "Photoinduced reactivity of titanium dioxide", Prog. Solid State Ch. 32(1-2), 33-177 (2004). http://dx.doi.org/10.1016/j.progsolidstchem.2004.08.001

[3] G. R. Dey, "Chemical reduction of CO_2 to different products during photo catalytic reaction on TiO_2 under diverse conditions: An overview", J. Nat. Gas Chem. 16(3), 217-226 (2007). http://dx.doi.org/10.1016/S1003-9953(07)60052-8

[4] K. Koč'ı, L. Obalová and Z. Lacný "Photocatalytic reduction of CO_2 over TiO_2 based catalysts", Chem. Pap. 62(1), 1-9 (2008). http://dx.doi.org/10.2478/s11696-007-0072-x

[5] A. L. Linsebigler, G. Lu and J. J. T. Yates, "Photocatalysis on TiO_2 surfaces: principles, mechanisms, and selected results", Chem. Rev. 95(3), 735-758 (1995). http://dx.doi.org/10.1021/cr00035a013

[6] J. Cyviene, D. Milcius and G. Laukaitis, "Porosity evaluation of TiO_2 thin films deposited using pulsed DC-magnetron sputtering", Mat. Sci. (Medziagotyra), 15(2), 103-107 (2009).

[7] B. B. F. Mirjalili and A. Akbari, "Nano-TiO_2: An eco-friendly alternative for the synthesis of quinoxalines", Chinese Chem. Lett. 22(6), 753-756 (2011). http://dx.doi.org/10.1016/j.cclet.2010.12.016

[8] M. C. Wu, A. Sápi, A. Avila, M. Szabó J. Hiltunen, M. Huuhtanen, G. Tóth, A. Kukovecz, A. Kónya, R. Keiski, W. F. Su, H. Jantunen and K. Kordás, "Enhanced photocatalytic activity of TiO_2 nanofibers and their flexible composite films: Decomposition of organic dyes and efficient H_2 generation from ethanol-water mixtures", Nano Res. 4(4), 360-369 (2011). http://dx.doi.org/10.1007/s12274-010-0090-9

[9] B. Reddy, G. Reddy, K. Rao, I. Ganesh and J. Ferreira, "Characterization and photocatalytic activity of TiO_2-M_xO_y (M_xO_y=SiO_2, Al_2O_3, and ZrO_2) mixed oxides synthesized by microwave-induced solution combustion technique", Mater. Sci. 44(18), 4874-4882 (2009). http://dx.doi.org/10.1007/s10853-009-3743-x

[10] S. Yang, W. Zhua, J. Wang and Z. Chen, "Catalytic wet air oxidation of phenol over CeO_2-TiO_2 catalyst in the batch reactor and the packed-bed reactor", J. Hazard. Mater. 153(3), 1248-1253 (2008). http://dx.doi.org/10.1016/j.jhazmat.2007.09.084

[11] J. Bandara, C. P. K. Udawatta and C. S. K. Rajapakse, "Highly stable CuO incorporated TiO_2 catalyst for

photocatalytic hydrogen production from H_2O", Photochem. & Photobiol.: Sciences 4(11), 857-861 (2005). http://dx.doi.org/10.1039/B507816D

[12] X. Zhang and L. Lei, "Preparation of photocatalytic Fe_2O_3-TiO_2 coatings in one step by metal organic chemical vapor deposition", Appl. Surf. Sci. 254(8), 2406-2412 (2008). http://dx.doi.org/10.1016/j.apsusc.2007.09.067

[13] L. Shi, C. Li, H. Gu and D. Fang, "Morphology and properties of ultrafine SnO_2-TiO_2 coupled semiconductor particles", Mater. Chem. Phys. 62(1), 62-67 (2000). http://dx.doi.org/10.1016/S0254-0584(99)00171-6

[14] T. Mishra, J. Hait, N. Aman, M. Gunjan, B. Mahato and R. K. Jana, "Surfactant mediated synthesis of spherical binary oxides photocatalytic with enhanced activity in visible light", Colloid Interf. Sci. 327(2), 377-383 (2008). http://dx.doi.org/10.1016/j.jcis.2008.08.040

[15] J. He, Q. Z. Cai, Q. Luo, D. Q. Zhang, T. T. Tang andY. F. Jiang, "Photocatalytic removal of methyl orange in an aqueous solution by a WO_3/TiO_2 composite film", Korean J. Chem.Eng. 27(2), 435-438 (2010). http://dx.doi.org/10.1007/s11814-010-0080-3

[16] Y. Zhao, C. Li, X. Liu, F. Gu, H. L. Du and L. Shi, "Zn-doped TiO_2 nanoparticles with high photocatalytic activity synthesized by hydrogen-oxygen diffusion flame", Appl. Catal. B-Environ. 79(3), 208-215 (2008). http://dx.doi.org/10.1016/j.apcatb.2007.09.044

[17] Y. Liu, H. Zhou, J. Li, H. Chen, D. Li, B. Zhou and W. Cai, "Enhanced photoelectrochemical properties of Cu_2O-loaded short TiO_2 nanotube array electrode prepared by sonoelectrochemical deposition", Nano-Micro Lett. 2(4), 277-284 (2010). http://dx.doi.org/10.3786/nml.v2i4.p277-284

[18] I. H. Tseng, W.-C. Chang and J. C. S. Wu, "Photoreduction of CO_2 using sol-gel derived titania and titania-supported copper catalysts", Appl. Catal. B: Environ. 37(1), 37-48 (2002). http://dx.doi.org/10.1016/S0926-3373(01)00322-8

[19] R. Lopez, R. Goez and M. E. Llanos, "Photophysical and photocatalytic properties of nanosized copper-doped titania sol-gel catalysts", Catal. Today 148(1-2), 103-108 (2009). http://dx.doi.org/10.1016/j.cattod.2009.04.001

[20] I. H. Tseng, J. C. S. Wu and H.-Y. Chou, "Effects of sol-gel procedures on the photocatalysis of Cu/TiO_2 in CO_2 photoreduction", J. Catalysis, 221(2), 432-440 (2004). http://dx.doi.org/10.1016/j.jcat.2003.09.002

[21] L. S. Yoong, F. K. Chong and B. K. Dutta, "Development of copper-doped TiO_2 photocatalyst for hydrogen production under visible light", Energy 34(10), 1652-1661, (2009). http://dx.doi.org/10.1016/j.energy.2009.07.024

[22] F. Boccuzzi, A. Chiorino, M. Manzoli, D. Andreeva, T. Tabakova, V. Ilieva and L. Iadakiev, "Gold, silver and copper catalysts supported on TiO_2 for pure hydrogen production", Catal. Today 75(1-4), 169-175 (2002). http://dx.doi.org/10.1016/S0920-5861(02)00060-3

[23] B. Zhu, Q. Guo, X. Huang, S. Wang, S. Zhang, S. Wu and W. Huang, "Characterization and catalytic performance of TiO_2 nanotubes-supported gold and copper particles", Mol. Catal. A: Chem. 249(1-2), 211-217 (2006). http://dx.doi.org/10.1016/j.molcata.2006.01.013

[24] B. Zhu, X. Zhang, S. Wang, S. Zhang, S. Wu and W. Huang, "Synthesis and catalytic performance of TiO_2 nanotubes-supported copper oxide for low-temperature CO oxidation", Micropor. Mesopor. Mat. 102(1-3), 333-336 (2007). http://dx.doi.org/10.1016/j.micromeso.2006.11.028

[25] T. Sato and M. Taya, "Copper-aided photosterilization of microbial cells on TiO_2 film under irradiation from a white light fluorescent lamp", Biochem. Eng. 30(2), 199-204 (2006). http://dx.doi.org/10.1016/j.bej.2006.04.002

[26] M. B. Fisher, D. A. Keane, P. Fernández-Ibánez, J. Colreavy, S. J. Hinder, K. G. McGuigan and S. C. Pilla, "Nitrogen and copper doped solar light active TiO_2 photocatalysts for water decontamination", Appl. Catal. B: Environ. 130-131, 8-13 (2013). http://dx.doi.org/10.1016/j.apcatb.2012.10.013

[27] B. Xin, P. Wang, D. Ding, J. Liu, Z. Ren and H. Fu, "Effect of surface species on Cu-TiO_2 photocatalytic activity", Appl. Surf. Sci. 254(9), 2569-2574 (2008). http://dx.doi.org/10.1016/j.apsusc.2007.09.002

[28] S. Watanabe, X. Ma and C. Song, "Selective sulfur removal from liquid hydrocarbon over regenerable CeO_2-TiO_2 adsorbent for fuel cell application", ACS: Div. Fuel Chem. 49(2), 511-513 (2004).

[29] B. B. Kefi, L. L. E. Atracheb, H. Kochkar anfd A. Ghorbel, "TiO_2 nanotubes as solid-phase extraction adsorbent for the determination of polycyclic aromatic hydrocarbons in environmental water samples", J. Environ. Sci. 23(5), 860-867 (2011). http://dx.doi.org/10.1016/S1001-0742(10)60481-0

[30] Y. Luo and D. Li, "Experimental study of nanometer TiO_2 for use as an adsorbent for SO_2 removal", Dev. Chem. Eng. Min. Process 10(3-4), 443-457 (2002). http://dx.doi.org/10.1002/apj.5500100414

[31] S. Deng, Z. Lia, J. Huang and G. Yua, "Preparation, characterization and application of a Ce–Ti oxide adsorbent for enhanced removal of arsenate from water", J. Hazard Mater. 179(1-3), 1014-1021 (2010). http://dx.doi.org/10.1016/j.jhazmat.2010.03.106

[32] S. J. Kim, E. G. Lee, S. D. Park, C. J. Jeon, Y. H. Cho, C. K. Rhee and W. W. Kim, "Photocatalytic effects of rutile phase TiO_2 ultrafine powder with high specific surface area obtained by a homogeneous precipitation process at low temperatures", Sol-Gel Sci. Tech. 22(1-2), 63-74 (2001). http://dx.doi.org/10.1023/A:1011264320138

[33] O. Zuas, H. Budiman and N. Hamim, "Anatase TiO_2 and mixed M-Anatase TiO_2 ($M = CeO_2$ or ZrO_2) nano powder: synthesis and characterization", I. J. Nano Dimens. 4(1), 11-18 (2013) In press.

[34] S. Martini and M. Herrera, "X-ray diffraction and crystal size", J. Am. Oil Chem. Soc. 79(3), 315-316 (2002). http://dx.doi.org/10.1007/s11746-002-0480-z

[35] Y. Masuda and K. Kato, "Synthesis and phase transformation of TiO_2 nano-crystal in aqueous solutions", Ceram. Soc. Jpn. 117(1363), 373-376 (2009). http://dx.doi.org/10.2109/jcersj2.117.373

[36] N. Sasirekha, S. J. S. Basha and K. Shanthi, "Photocatalytic performance of Ru doped anatase mounted on silica for reduction of carbon dioxide", Appl. Catal. B: Environ. 62(1), 169-180 (2006). http://dx.doi.org/10.1016/j.apcatb.2005.07.009

[37] L. Ge, M. Xu, M. Sun and H. Fang, "Low-temperature synthesis of photocatalytic TiO_2 thin film from aqueous anatase precursor sols", J. Sol-Gel Sci. Techn. 38(1), 47-53 (2006). http://dx.doi.org/10.1007/s10971-006-6009-y

[38] S. R. Dhage, S. P. Gaikwad anfd V. Ravi, "Synthesis of nanocrystalline TiO_2 by tartarate gel method",

B. Mater. Sci. 27(6), 487-489 (2004). http://dx.doi.org/10.1007/BF02707273

[39] O. Vázquez-Cuchillo, A. Cruz-López, L. M. Bautista-Carrillo, A. Bautista-Hernández, L. M. Torres Martínez and S. W. Lee, "Synthesis of TiO_2 using different hydrolysis catalysts and doped with Zn for efficient degradation of aqueous phase pollutants under UV light", Chem. Intermediet. 36(1), 103-113 (2010). http://dx.doi.org/10.1007/s11164-010-0119-4

[40] R. López, R. Gómez andf M. E. Llanos, "Photophysical and photocatalytic properties of nanosized copper-doped titania sol-gel catalysts", Catal. Today 148(1-2), 103-108 (2009). http://dx.doi.org/10.1016/j.cattod.2009.04.001

[41] M. Sabzi, S. M. Mirabedini, J. Zohuriaan-Mehr and M. Atai, "Surface modification of TiO_2 nano-particles with silane coupling agent and investigation of its effect on the properties of polyurethane composite coating", Progr. Org. Coating. 65(2), 222-228 (2009). http://dx.doi.org/10.1016/j.porgcoat.2008.11.006